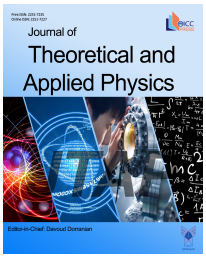

Volume 18, Issue 2, 182422 (1-7)

Journal of Theoretical and Applied Physics (JTAP)

https://dx.doi.org/10.57647/j.jtap.2024.1802.22

Adsorption and release of thymol using metal organic framework $Zn_2(BDC)_2(DABCO)$ and its chitosan nanocomposite

Negar Motakef Kazemi*, Mahdieh Ghorbani

Department of Medical Nanotechnology, Faculty of Advanced Sciences and Technology, Tehran Medical Sciences, Islamic Azad University, Tehran, Iran.

***Corresponding author:** motakef@iaups.ac.ir

Original Research

Received:
24 November 2023
Revised:
29 December 2023
Accepted:
4 January 2024
Published online:
10 March 2024

Abstract:

Metal organic frameworks (MOFs) are new drug delivery systems because they have large surface area, tunable pore sizes, and controlled drug release. In the present work, $Zn_2(BDC)_2(DABCO)$ MOF is prepared by a quick and simple method. Then, thymol is loaded into MOF (thymol@MOF) and its chitosan (MOF-CH) at room temperature. And finally, the release of thymol from two samples is investigated. Chitosan polymer has been modified the MOF to develop an efficient adsorbent for the first time and controlled release. The samples were characterized by Fourier transform infrared (FTIR) spectroscopy for determination of functional groups, X-ray diffraction (XRD) for evaluation of crystal structure, field emission scanning electron microscope (FESEM) for investigation of morphology and size, and ultraviolet-visible (UV-Vis) spectroscopy for evaluation of thymol amount. The antibacterial activity of samples was investigated by *Escherichia coli* (*E. coli*) as gram-negative bacterium and *Staphylococcus aureus* (*S. aureus*) as gram-positive bacterium. Based on the results, thymol was successfully encapsulated in MOF and MOF-CH, and the samples have high-efficiency antibacterial activity.

Keywords: Antibacterial activity; Metal organic framework; Thymol; $Zn_2(BDC)-2(DABCO)$ MOF

1. Introduction

Thymol is a monoterpene phenol with antifungal, antioxidant and antibacterial activities [1]. Due to the presence of phenolic hydroxyl group in its structure, thymol is able to destroy the membrane of Gram-negative bacteria and disturb the balance of mineral ions and pH homeostasis inside the cytoplasm of prokaryotic cells. Also, a low concentration of thymol inhibited the release of enterotoxin in *Staphylococcus aureus* as gram-positive bacterium [2]. The limitation of the use of thymol is due to its low solubility in water and the reduction of its contact with the bacteria in water and, as a result, its inhibition efficiency. Therefore, the expansion of thymol nanocarriers is important [3]. Chitosan is a linear polysaccharide that has various applications due to its unique solubility as well as chemical and biological properties. This compound has many active amino side groups that allow chemical modification and creation of a wide range of useful derivatives [4]. Chitosan nanoparticles have been widely investigated for drug delivery due to their biodegradability, biocompatibility, and low toxicity [5].

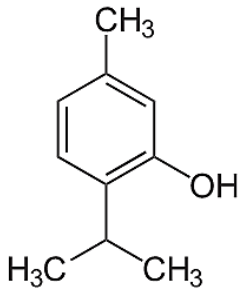

Figure 1. Structure of thymol.

MOFs have recently attracted much attention as a new

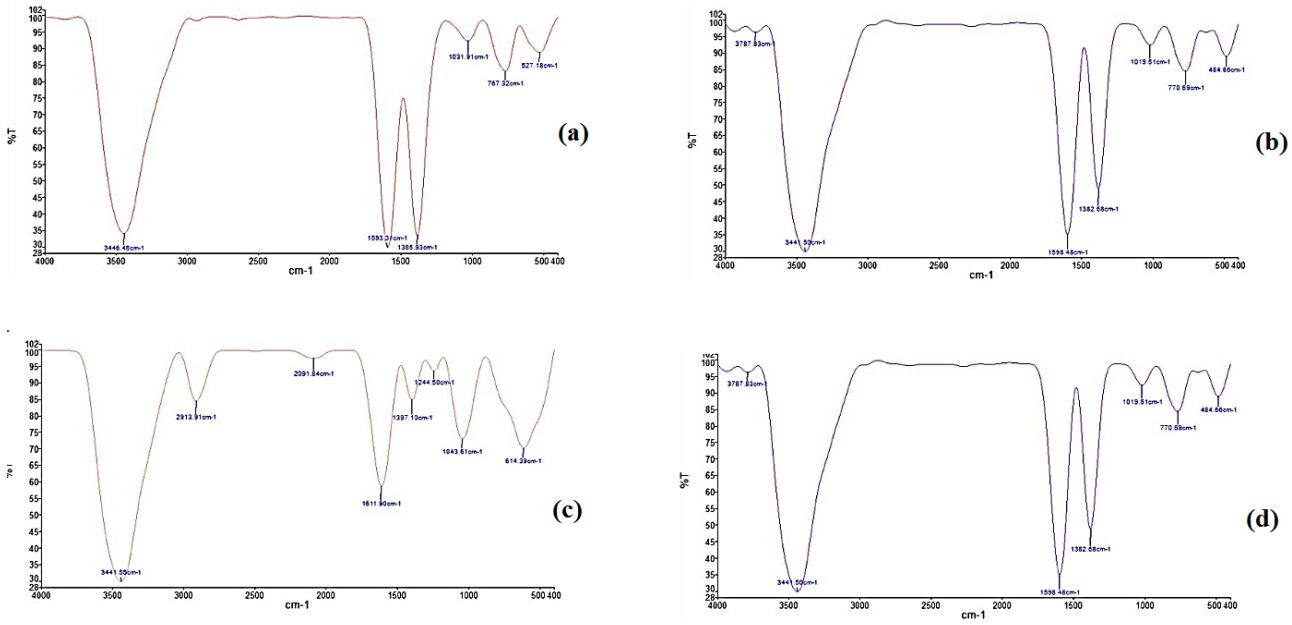

Figure 2. FTIR spectrum of (a) MOF, (b) thymol@MOF, (c) MOF-CH, and (d) thymol@MOF-CH.

class of hybrid materials consisting of the self-assembly of metal ions (or clusters) as metal centers and ligands as linkers [6]. These compounds are synthesized by various methods including hydrothermal [7], solvothermal [8], solution [9], ionic liquids [10], son chemical [11], microwave [12], electrochemical [13], diffusion [14], mechanochemical [15], laser ablation [16], combination of ultrasound and microwave [17]. Nowadays, the use of MOF as nanocarriers [18, 19] and compounds with antibacterial activity [20] has been expanded. Recently, there have been reports on thymol loading in MOFs [21, 22]. $Zn_2(BDC)_2(DABCO)$ is a zinc metal-based MOF (Zn-MOF) with nanocarrier applications. This MOF is synthesized by self-assembly of Zn_4O units as metal center and ,4-benzenedicarboxylate and 1,4-diazabicyclo [2.2.2] octane ligands as linker and bridge [23]. $Zn_2(BDC)_2(DABCO)$ MOF can be synthesized by solution and solvothermal method [24, 25]. In the present study, according to functional groups, $Zn_2(BDC)_2(DABCO)$ MOF was investigated as a suitable candidate for thymol absorption. The novelty and objectives of the article are to investigate the possibility of encapsulation and release of thymol as an environmentally friendly volatile antimicrobial

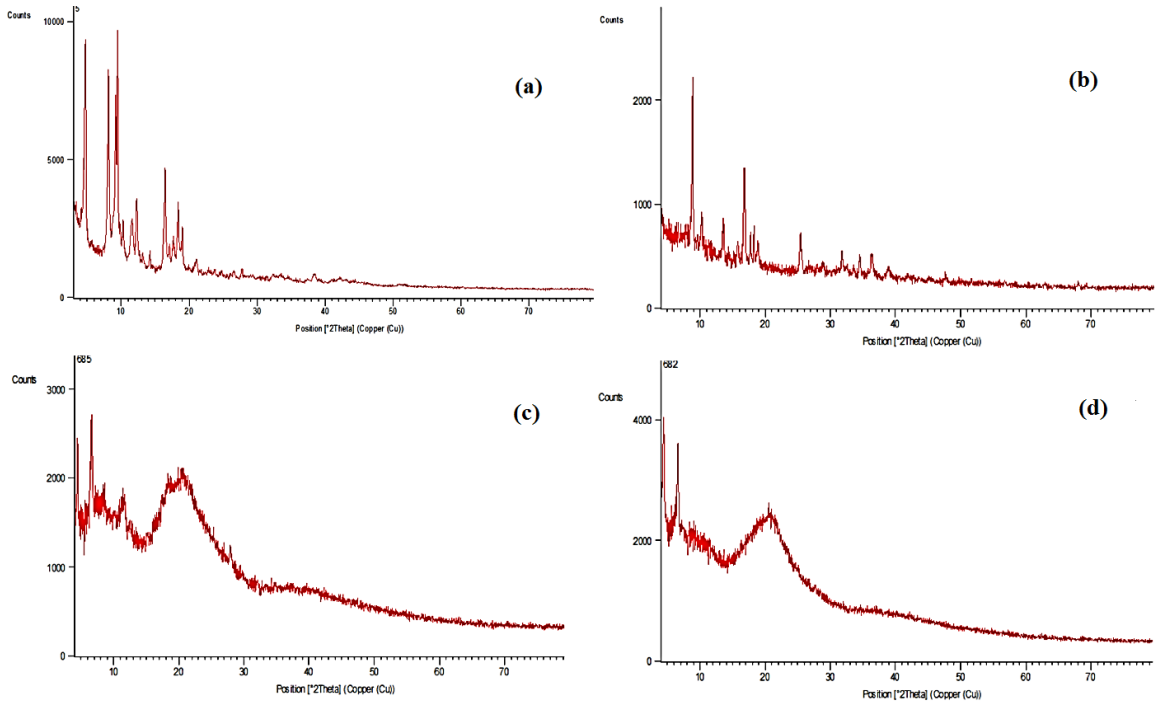

Figure 3. XRD pattern of (a) MOF, (b) thymol@MOF, (c) MOF-CH, and (d) thymol@MOF-CH.

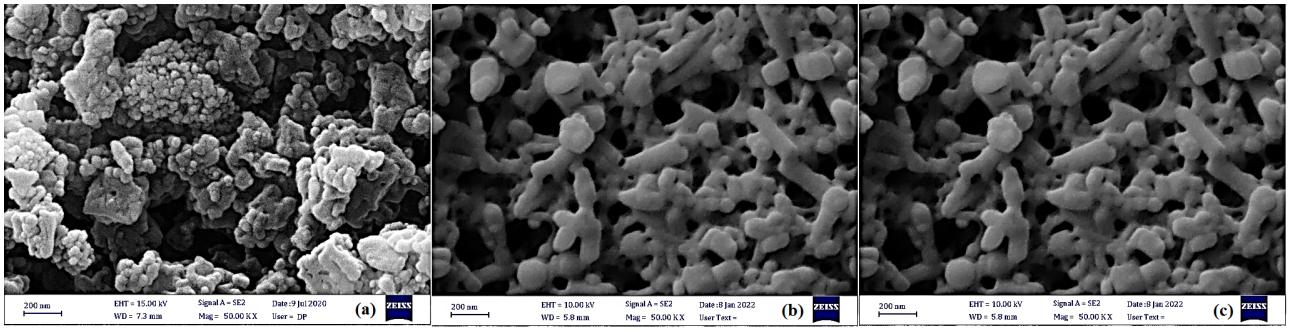

Figure 4. FESEM images of (a) MOF, (b) MOF-CH, and (c) thymol@MOF-CH.

essential oil based on the structure and interactions of pi-pi stacking and hydrogen bond.

2. Experimental procedure

All materials used in this study, including thymol, dimethylformamide (DMF), Zn acetate dehydrate ($Zn(OAc)_2.2H_2O$), 1,4 benzene dicarboxylic acid, 1, 4 diazabicyclo [2.2.2] octane, and phosphate-buffered saline (PBS), were purchased from Merck Company (Germany), and the distilled water used in this research was the distilled water machine of the Pharmaceutical Sciences Laboratory of Islamic Azad University, Tehran, Iran.

The MOF was prepared by using 0.132 g of Zn acetate dehydrates as the metal center, 0.1 of 1, 4 benzene dicarboxylic acid as the bridging ligand, and 0.035 g of 1, 4 diazabicyclo [2.2.2] octane as the chelating ligand in 25 mL DMF as the solvent under reflux for 30 min at room temperature [24]. The white crystals were rinsed with DMF for removing the remaining ligand and metal and dried under vacuum for 6 hours at 120º C.

To load thymol in the MOF, 5 mL of thymol (100 ppm thymol in the water solution) was added to white MOF crystals (50 mg). The reactants were sealed and stirred at 300 rpm for 30 minutes at room temperature. The solution was centrifuged at 15000 rpm for 10 minutes and dried under vacuum for 6 hours at 60º C. Finally, thymol-MOF was coated with a 2 W% chitosan solution in 2 V% acetic acid, and purified using filtration and dried in a vacuum oven for 6 h at 60º C. According to the structure of thymol (Fig. 1) and MOF [26] and the presence of hydroxyl group and benzene ring in these compounds, hence the interactions of pi-pi stacking and hydrogen bond are the main factors of drug loading according to previous articles [24, 25].

The samples were characterized by FTIR, XRD, FESEM, and UV-Vis spectroscopy. Fourier transform infrared spectroscopy was used to determine the chemical bonds of samples by Spectrum Two FTIR Spectrometer from PerkinElmer. X-ray diffraction pattern was employed for investigation of crystalline structures of samples by of dried suspensions on Si substrate. X-ray diffraction patterns were recorded by STOE X-ray diffractometer with Cu Kα radiation ($\lambda = 1.54060$ Å). Morphology and size of samples were evaluated by FESEM (SIGMA VP) microscopes from Zeiss Company. UV-Vis spectroscopy was employed to evaluate the thymol at the maximum wavelength with the Shimadzu model UV-1700 PharmaSpec. The antibacterial activity was evaluated by disk diffusion method against *Escherichia coli* as gram-negative bacteria (ATCC 25922) and *Staphylococcus aureus* as gram-positive bacteria (ATCC 25923) by measuring the zone inhibition and minimum inhibitory concentration (MIC).

3. Results and discussion

FTIR spectra of the samples are shown in Fig. 2 in the range of $400 - 4000$ cm^{-1} with KBr pellets. For pure MOF, the absorption peak at $2900 - 3800$ cm^{-1} is due to alkyl C–H, amine O–H, and N–H stretching. In addition, the high and clear intensity peak at 1628 cm^{-1} is assigned to

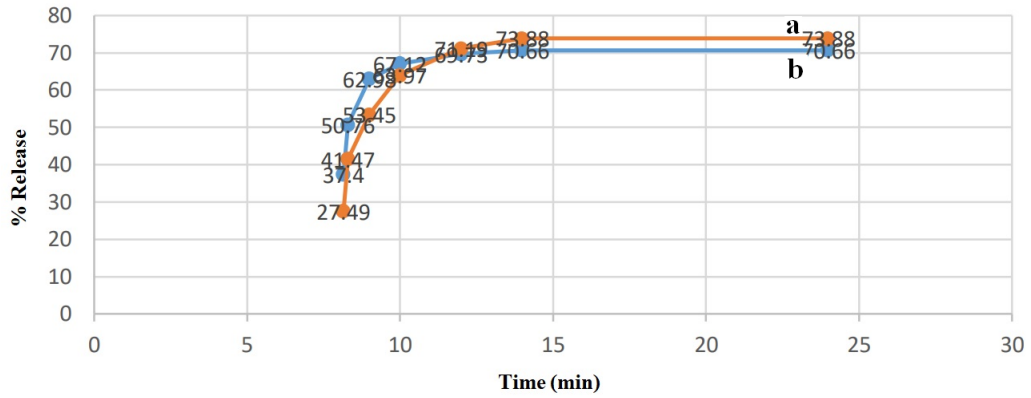

Figure 5. Percentage of the cumulative thymol release from (a) MOF and (b) MOF-CH.

Table 1. The zone inhibition and MIC

Sample	Zone inhibition *E. coli* (mm)	MIC *S. aureus* (mg/mL)	Zone inhibition *E. coli* (mm)	MIC *S. aureus* (mg/mL)
Thymol	8	3	7	2
MOF	9	1	8	1
Thymol@MOF	11	1	10	1
MOF-CH	21	0.056	20	0.562
Thymol@MOF-CH	25	0.056	23	0.562

C=O stretching. At 1390 cm^{-1}, the high intensity peak of C=O belongs to the carboxylic acid groups. It was revealed that the peak at 2370 cm^{-1} corresponds to environment CO_2. The C=C stretching of the aromatic bands is observed at 1582 cm^{-1}. The peaks at 1582, 1136, 1100, 819, and 746 cm^{-1} are assigned with N–C–H compound of DABCO. The results confirm the previous report [24, 25]. For thymol, the peak at $3550 - 3200$ cm^{-1} is assigned with alcohol/phenol O-H stretch. The C-H(aromatic) is assigned at $3150 - 3050$ cm^{-1}. The aromatic c=c stretch is assigned at ~ 1500 cm^{-1}. The CHx deformation band is specified at $1500 - 1400$ cm^{-1}. The results confirm the previous report [27, 28]. For chitosan, the strong band at ~ 3300 cm^{-1} is corresponded to N-H and O-H stretching. The C-H symmetric and asymmetric stretching are observed at around 2921 and 2877 cm^{-1}, respectively. The C=O stretching of amide I is observed at around ~ 1645 cm^{-1}. The C-N stretching of amide III is assigned at 1325 cm^{-1}. The N-H bending of the primary amine is observed at 1589 cm^{-1}. The CH_2 bending and CH_3 symmetrical deformations are confirmed by the presence of bands at around 1423 and 1375 cm^{-1}, respectively. The peak at 1153 cm^{-1} is attributed to asymmetric stretching of the C-O-C bridge. The band at ~ 1080 cm^{-1} is corresponded to C-O stretching. The results confirm the previous report [29, 30]. FTIR analysis qualitatively shows the functional groups.

X-ray diffraction patterns of nanostructures in the range of $2\theta = 5°$ - $80°$ are presented in Fig. 3. The XRD pattern of the MOF is similar to the previous report and the crystalline structure is preserved after the adsorption based on the previous report [24, 25]. The XRD of chitosan approved the crystalline structure according to the previous report with two characteristic peaks at $2\theta = 10°$ and $20°$ [30]. Therefore, the presence of chitosan reduces the crystal structure. Based on the results, thymol has a crystalline structure [31, 32], and the crystalline structure is reduced due to thymol loading in samples.

FESEM shows shape and size in Fig. 4. Based on these results, the size increases slightly with the increase of thymol and chitosan.

The percentage of the released thymol from MOF and MOF-CH in PBS at 37° C and pH 7.4 [33–35] is shown in Fig. 5. The thymol concentration of the sample was analyzed by UV-Vis spectroscopy. Based on the loading mechanism and release diagram, the drug is loaded in the MOF. According to the results, the presence of chitosan causes a slight increase in the percentage of thymol release. Because chitosan covers the MOF and limits the holes in drug release [36–39]. Therefore, the controlled release system was obtained by increasing the release time of thymol in the presence of chitosan.

The zone inhibition and MIC are shown in Table 1. The medium was used overnight for the growth of *Staphylococcus aureus* and *Escherichia coli* at 37° C for 24 h. Based on the results, the presence of chitosan and thymol increased the antibacterial activity. The results confirm the previous reports [40–42].

4. Conclusion

In this study, thymol was entrapped in the $Zn_2(BDC)_2(DABCO)$ and coated with CH for DDS. Also, these samples showed good release performance of thymol in PBS at pH 7.4. Its structural properties were characterized by FTIR, XRD, and FESEM. The release of thymol from the samples was confirmed by UV-Vis spectroscopy. The samples showed good antibacterial activity against *E. coli* as gram-negative bacteria and *S. aureus* as gram-positive bacteria. Based on the results, the presence of chitosan and thymol has a great effect in increasing antibacterial activity. Therefore, the future perspective based on these compounds can have a good potential for the development of their antibacterial application.

Ethical approval
This manuscript does not report on or involve the use of any animal or human data or tissue. So the ethical approval is not applicable.

Authors Contributions
All the authors have participated sufficiently in the intellectual content, conception and design of this work or the analysis and interpretation of the data (when applicable), as well as the writing of the manuscript.

Availability of data and materials
Data presented in the manuscript are available via request.

Conflict of Interests
The author declare that they have no known com-

peting financial interests or personal relationships that could have appeared to influence the work reported in this paper.

References

[1] M. I. Alvarez Echazú, C. E. Olivetti, C. Anesini, C. J. Perez, G. S. Alvarez, and M. F. Desimone. "Development and evaluation of thymol-chitosan hydrogels with antimicrobial-antioxidant activity for oral local delivery.". *Mater. Sci. Eng. C.*, **81**:588–596, 2017.

[2] Y. Wu, Y. Luo, B. Zhou, M. Lei, Q. Wang, and B. Zhang. "Porous metal-organic framework (MOF) Carrier for incorporation of volatile antimicrobial essential oil. ". *Food Control*, **98**:174–178, 2019.

[3] A. Escobar, M. Pérez, G. Romanelli, and G. Blustein. "Thymol bioactivity: A review focusing on practical applications. ". *Arabian Journal of Chemistry*, **12**: 9243–69, 2020.

[4] M. A. Ibrahim, M. H. Alhalafi, E. A. M. Emam, H. Ibrahim, and R. M. Mosaad. "A review of chitosan and chitosan nanofiber: Preparation, characterization, and its potential applications. ". *Polymers*, **15**:2820, 2023.

[5] R. Jha and R. A. Mayanovic. "A review of the preparation, characterization, and applications of chitosan nanoparticles in nanomedicine. ". *Nanomaterials*, **13**: 1302, 2023.

[6] M. Ma, J. Chen, H. Liu, Z. Huang, F. Huang, Q. Lia, and Y. Xu. "A review on chiral metal–organic frameworks: synthesis and asymmetric applications. ". *Nanoscale*, **14**:13405–427, 2022.

[7] T. Sattar and M. Athar. "Hydrothermal synthesis and characterization of copper glycinate (Bio-MOF-29) and it's in vitro drugs adsorption studies.". *J Inorg Chem.*, **7**:17–27, 2017.

[8] B. Zhang, Y. Luo, K. Kanyuck, N. Saenz, K. Reed, P. Zavalij, J. Mowery, and G. Bauchan. "Facile and template-free solvothermal synthesis of mesoporous/-macroporous metal–organic framework nanosheets.". *RSC Adv.*, **8**:33059–64, 2018.

[9] D. J. Tranchemontagne, R. J. Hunt, and O. Yaghi. "Room temperature synthesis of metal-organic frameworks: MOF-5, MOF-74, MOF-177, MOF-199, and IRMOF-0.". *Tetrahedron*, **64**:8553–57, 2008.

[10] J. H. Liao, P. C. Wu, and W. C. Huang. "Ionic liquid as solvent for the synthesis and crystallization of a coordination polymer: (EMI)[Cd(BTC)] (EMI = 1-Ethyl-3-methylimidazolium, BTC = 1,3,5- benzenetricarboxylate).". *Cryst Growth Des.*, **6**:1062–63, 2006.

[11] W. J. Son, J. Kim, J. Kim, and W. S. Ahn. "Sonochemical synthesis of MOF-5. ". *Chem Commun.*, **47**: 6336–38, 2008.

[12] S. H. Jhung, J. H. Lee, J. W. Yoon, C. Serre, G. Ferey, and J. S. Chang. "Microwave synthesis of chromium terephthalate MIL-101 and Its benzene sorption.". *Adv Mater.*, **19**:121–124, 2007.

[13] H. M. Yang, X. Liu, X. L. Song, T. L. Yang, Z. H. Liang, and C. M. Fan. "In situ electrochemical synthesis of MOF-5 and its application in improving photocatalytic activity of BiOBr.". *T Non ferr Metal Soc.*, **25**:3987–94, 2015.

[14] Y. Chen, C. Yang, X. Wang, J. Yang, K. Ouyang, and J. Li. "Kinetically controlled ammonia vapor diffusion synthesis of a Zn(II) MOF and its H_2O/NH_3 adsorption properties.". *J Mater Chem A.*, **4**:10345–351, 2016.

[15] D. Lv, Y. Chen, Y. Li, R. Shi, H. Wu, X. Sun, J. Xiao, H. Xi, Q. Xia, and Z. Li. "Efficient mechanochemical synthesis of MOF-5 for linear alkanes adsorption. ". *J. Chem Eng Data.*, **62**:2030–36, 2017.

[16] S. L. Campello, G. Gentil, S. A. Júnior, and W. M. de Azevedo. "Laser ablation: a new technique for the preparation of metal-organic frameworks $Cu_3(BTC)_2(H_2O)_3$. ". *Mater.*, **148**:200–203, 2015.

[17] R. Sabouni, H. Kazemian, and S. Rohani. "A novel combined manufacturing technique for rapid production of IRMOF-1 using ultrasound and microwave energies.". *Chem Eng J.*, **165**:966–973, 2010.

[18] Z. Zong, G. Tian, J. Wang, C. Fan, F. Yang, and F. Guo. "Recent advances in metal–organic-framework-based nanocarriers for controllable drug delivery and release.". *Pharmaceutics*, **14**:2790, 2022.

[19] M. Moharramnejad, A. Ehsani, M. Shahi, S. Gharanli, H. Saremi, R. Es'haghi Malekshah, Z. Salmanivand Basmenj, S. Salmani, and M. Mohammadi. "MOF as nanoscale drug delivery devices: Synthesis and recent progress in biomedical applications.". *Journal of Drug Delivery Science and Technology.*, **81**:104285, 2023.

[20] J. Liu, D. Wu, N. Zhu, Y. Wu, and G. Li. "Antibacterial mechanisms and applications of metal-organic frameworks and their derived nanomaterials.". *Trends Food Sci. Technol.*, **109**:413–434, 2021.

[21] Z. Li, Y. Sun, X. Pan, T. Gao, T. He, C. Chen, B. Zhang, X. Fu, and Q. Huang. "Controlled release of thymol by cyclodextrin metal-organic frameworks for preservation of cherry tomatoes. ". *Foods*, **11**:3818, 2022.

[22] D. Ganta, C. Guzman, K. Combrink, and M. Fuentes. "Adsorption and removal of thymol from water using a zeolite imidazolate framework-8 nanomaterial.". *Analytical Letters*, **54**:625–636, 2021.

[23] Y. Kim, R. Haldar, H. Kim, J. Kooac, and K. Kim. "The guest-dependent thermal response of the flexible MOF Zn2(BDC)2(DABCO).". *Dalton Trans.*, **45**: 4187–92, 2016.

[24] N. Motakef-Kazemi, S. A. Shojaosadati, and A. Morsali. "In situ synthesis of a drug-loaded MOF at room temperature. ". *Micropor Mesopor Mat.*, **186**:73–79, 2014.

[25] N. Motakef-Kazemi, S. A. Shojaosadati, and A. Morsali. "Evaluation of the effect of nanoporous nanorods Zn2(bdc)2(dabco) dimension on ibuprofen loading and release.". *J. Iran. Chem. Soc.*, **13**:1205–12, 2016.

[26] F. Ghourchian, N. Motakef-Kazemi, E. Ghasemi, and H. Ziyadid. "Zn-based MOF-chitosan-Fe_3O_4 nanocomposite as an effective nano-catalyst for azo dye degradation. ". *J. Environ. Chem. Eng.*, **9**:106388, 2021.

[27] H. Schulz, G. Ozkan, M. Baranska, H. Kruger, and M. Ozcan. "Characterisation of essential oil plants from Turkey by IR and Raman spectroscopy.". *Vib Spectrosc.*, **39**:249–56, 2005.

[28] H. Schulz, R. Quilitzsch, and H. Kruger. "Rapid evaluation and quantitative analysis of thyme, origano and chamomile essential oils by ATR-IR and NIR spectroscopy.". *J Mol Struct.*, **661–662**:299–306, 2003.

[29] M. Fernandes Queiroz, K. Rachel Teodosio Melo, D. Araujo Sabry, G. Lanzi Sassaki, and H. Alexandre. "Oliveira Rocha does the use of Chitosan contribute to oxalate kidney stone formation?". *Mar. Drugs.*, **13**: 141–158, 2015.

[30] M. Morsy, K. Mostafa, H. Amyn, A. Abdel hameed El-Ebissy, A. Mohamed Salah, and M. Adel Youssef. "Synthesis and characterization of freeze dryer chitosan nano particles as multi-functional eco-friendly finish for fabricating easy care and antibacterial cotton textiles.". *Egypt. J. Chem.*, **62**:1277–93, 2019.

[31] W. Zhou, Y. Zhang, R. Li, S. Peng, R. Ruan, J. Li, and W. Liu. "Fabrication of caseinate stabilized thymol nanosuspensions via the pH-driven method: Enhancement in water solubility of thymol.". *Foods*.

[32] A. Mohamed Mohsen, Y. Ibrahim Nagy, A. M. Shehabeldine, and M. M. Okba. "Thymol-loaded eudragit RS30D cationic nanoparticles-based hydrogels for topical application in wounds: In vitro and in vivo evaluation.". *Pharmaceutics*, **15**:19, 2023.

[33] S. Sanaei-Rad, M. Ali Ghasemzadeh, and S. M. Hossein Razavian. "Synthesis of a novel ternary ZIF-8/GO/$MgFe_2O_4$ nanocomposite and its application in drug delivery. ". *Scientific Reports*, **11**:18734, 2021.

[34] M. Nasrabadi, M. A. Ghasemzadeh, and M. R. Zand Monfared. "The preparation and characterization of UiO-66 metal–organic frameworks for the delivery of the drug ciprofloxacin and an evaluation of their antibacterial activities.". *New J. Chem.*, **43**:16033–40, 2019. DOI: https://doi.org/10.1039/C8RA06576D.

[35] M. Esfahanian, M. A. Ghasemzadeh, and S. M. Hossein Razavian. "Synthesis, identification and application of the novel metal-organic framework Fe_3O_4@PAA@ZIF-8 for the drug delivery of ciprofloxacin and investigation of antibacterial activity.". *Artificial Cells, Nanomedicine, and Biotechnology*, **47**:2024–30, 2019.

[36] L. Li, S. Han, S. Zhao, X. Li, B. Liu, and Y. Liu. "Chitosan modified metal–organic frameworks as a promising carrier for oral drug delivery. ". *RSC Adv.*, **10**:45130–38, 2020.

[37] E. Aghazadeh Asl, M. Pooresmaeil, and H. Namazi. "Chitosan coated MOF/GO nanohybrid as a co-anticancer drug delivery vehicle: Synthesis, characterization, and drug delivery application. ". *Materials Chemistry and Physics*, **293**:126933, 2023.

[38] M. Akbari, M. A. Ghasemzadeh, and M. Fadaeian. "Synthesis and application of ZIF-8 MOF incorporated in a TiO_2@chitosan nanocomposite as a strong nanocarrier for the drug delivery of acyclovir.". . *Chemistry Europe.*, **5**:14564–71, 2020.

[39] M. Parsaei and K. Kamran Akhbari. "Synthesis and application of MOF-808 decorated with folic acid-conjugated chitosan as a strong nanocarrier for the targeted drug delivery of quercetin.". *Inorg Chem.*, **61**: 19354–68, 2022.

[40] S. Sreelatha, N. Kumar, T. Si Yin, and S. Rajani. "Evaluating the antibacterial activity and mode of action of thymol-loaded chitosan nanoparticles against plant bacterial pathogen Xanthomonas campestris pv. Campestris.". *Front Microbiol*, **12**:792737, 2021.

[41] S. Sreelatha, N. Kumar, and S. Rajani. "Biological effects of Thymol loaded chitosan nanoparticles (TCNPs) on bacterial plant pathogen Xanthomonas campestris pv. Campestris.". *Front. Microbiol. Sec. Microbiotechnology*, **13**:2022, 2022.

[42] E. Medina, N. Caro, L. Abugoch James, A. Gamboa, M. Díaz Dosque, and C. Tapia. "Chitosan thymol

nanoparticles improve the antimicrobial effect and the water vapour barrier of chitosan-quinoa protein films.”. *Journal of Food Engineering*, **240**:191–198, 2019.